Measurement: Sensors 7-9 (2020) 100014

Contents lists available at ScienceDirect

Measurement: Sensors

journal homepage: www.journals.elsevier.com/measurement

Flow distribution imaging and sensing for leaks in pipelines using decimated signal diagonalization

Aimé Lay-Ekuakille [a,*], Vito Telesca [b]

[a] Department of Innovation Engineering, University of Salento, Lecce, Italy
[b] School of Engineering, University of Basilicata, Potenza, Italy

ARTICLE INFO

Keywords:
Decimated signal Diagonalization
Leak detection in pipelines
3D imaging and sensing
Pressure sensors
Spectral analysis
Flow measurement
Nuclear magnetic imaging

ABSTRACT

Control and monitoring of pipelines, dedicated to liquids transportation and distribution, are generally performed by active and passive techniques. With active techniques, we intend the possibility of using external sources to target pipelines and/or liquid inside the infrastructure. The used radiation can be partly reflected by the liquid and pipeline. Passive techniques are related to spontaneous emissions from liquids within the pipelines. However, capturing water displacements and fluctuations within the pipeline, by means of sensors and transducers, is somehow a passive technique. This latter is here illustrated thanks to pressure sensors mounted on an experimental pipeline. The basic idea is to detect leaks but also to monitor water flow regime by means of imaging without using a camera. That is possible thanks to the algorithm here developed and based on 2D/3D Decimated Signal Diagonalization (DSD). It is a technique used in nuclear magnetic resonance, and susceptible to bring to excellent results if water flow within a pipeline is considered as blood flow inside an artery or a vein. The approach has been applied to an experimental hydraulic circuit.

1. Introduction

Water distribution is a key issue of any economy and human society because of its great impact on any activity. The loss of water, during its transportation and distribution, is one of the big challenges of any country, region and city. Losses also determine the cost of water distribution and its increasing economic burden. In many western countries, attention is greatly paid on loss along pipelines, such as waterworks, and the following rules have to be considered:

- loss < 10%, acceptable, monitoring and control are performed;
- loss 10%–25%, intermediate, and could be reduced;
- loss> 25%, is a matter of concerns, then draconian reduction is necessary.

Fig. 1 depicts losses distributed per country in the European Union. The Netherlands exhibits a lowest average distribution loss (around 3–4%) than the other countries. The highest level is related to Ireland (around 47%). However, the mean value, for EU countries, is 23% of losses [1].

Manifold reasons of losses are reported in Fig. 2 where we observe different components that arise such as pipe breaks and leaks [2]. These are the reasons of monitoring and control of the pipe faced in this paper.

Within the above reasons we encompass quality of materials used to manufacture junctures and pipes, low level of maintenance, random damages, erroneous operating pressure loss, and damages due to external works on the pipe or close to the pipe. Leak mechanism is explained in Fig. 3 in which changes of pressure generate wave front reflections with increasing of damped wave from a downstream point, with respect to the specific leak point, and a reverse wave looking for a point where water can come out. Reflections create turbulence that produces the decay rate of the transient signal. The decay process is forward exploited for spectral estimation.

Since the main scope of the paper is focused on spectral estimation, we recall papers' authors dealing with [3–5]. A particular series of techniques exploiting NMR (Nuclear Magnetic Resonance), thanks to decaying process, is used since it allows to be used here as it is for detecting blood flow in arteries and veins. The techniques, included in the series, are considered as advanced transforms permitting changes of references from time domain to frequency domain. They fit in with sensor signal processing and high resolution-based signal treatment. The main transforms used in leak detection in pipelines are: FDM (Filter Diagonalization Method) [6,7], DPA (Decimated Padé Approximant) [8,9] and DSD (Decimated Signal Diagonalization) [10]. All the above

* Corresponding author.
E-mail address: aime.lay.ekuakille@unisalento.it (A. Lay-Ekuakille).

https://doi.org/10.1016/j.measen.2020.100014
Received 15 March 2019; Received in revised form 6 May 2020; Accepted 1 September 2020
Available online 15 September 2020

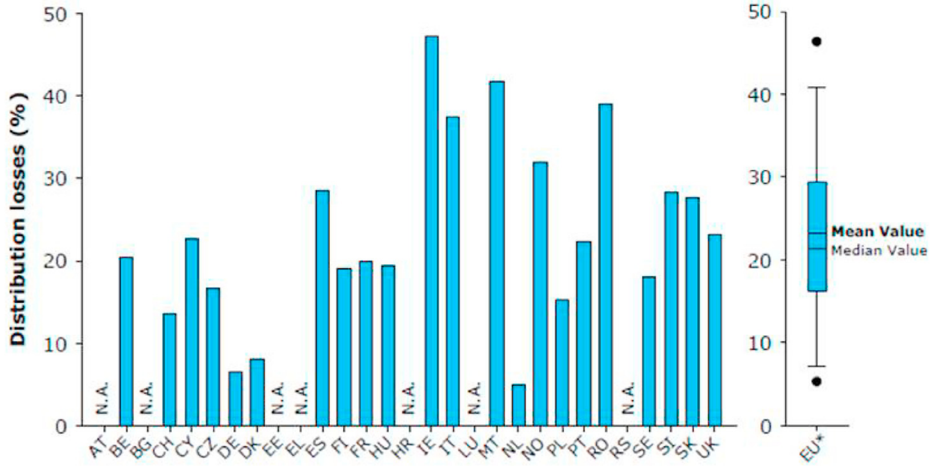

Fig. 1. Average distribution of losses in percentages in EU countries.

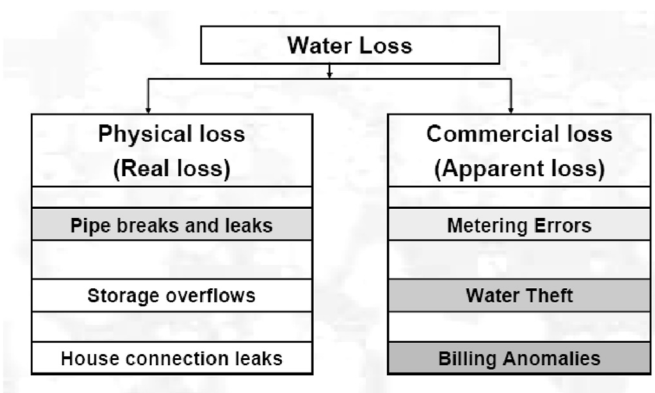

Fig. 2. Components of water loss in a waterworks system.

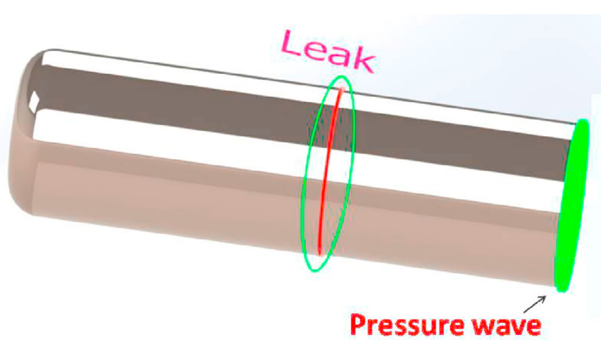

Fig. 3. Leak mechanism in a pipe and pressure variation.

transforms can be employed for 2D/3D representation.

2. Multidimensional decimated signal diagonalization

Decimated Signal Diagonalization is one of the techniques used in NMR allowing transformation of references from time domain into frequency domain. It allows to carried out a spectroscopy of water molecules within the human body. NMR spectroscopy and MRI (Magnetic Resonance Imaging) are employed to observe signals coming from various nuclei, in particular from protons (^{1}H) of water molecules. MRI basically adopts a spatial coding that allows to assign to each signal a precise location on a plane or within a volume, and retrieves images. This coding contains two components: the frequency coding (of our interest) and the phase coding. Given two objects X and Y that resonate at the same frequency ν_0 within a homogeneous magnetic field B_0; the received signal, after Fourier transform (FT), will deliver a resonance amplitude which surface will be proportional to the total number of resonating nuclei of both objects. This situation is described in Fig. 4 (left).

Conversely, if these two objects are under a non-homogeneous field B_0 corresponding to a gradient $\Delta\ B_0$ according to the direction $0x$, the object X will be under a field B_{0x} and the object Y to a field B_{0y}. The resonating frequencies ν_{0x} and ν_{0y} will be then different, and the FT will deliver two separate amplitudes with a displacement proportional to the distance d that separates X from Y (Fig. 4 right). Features represented in Fig. 4 clearly justify the use of frequency domain to "discover" and "search" for peaks that may reflect protons in water molecules. Now to detect interested peaks of flow we need a detector (sensor) able to capture useful frequencies. To understand this idea, let us recall one of the first experiments in NMR for flow measurement [11] as reported in Fig. 5, and subsequently confirmed by different authors [12]. Excitation should be considered as the event of leak that changes flow regime within the pipe as flow within the artery/vein. The detector (left), as sensor, reveals the peak and normal flow. By modifying the distance between two antennas (sensors), see Fig. 5 (right), the range of measurable flows is major.

That is why a certain number of pressure sensors should be mounted on the pipeline to capture more peaks. DSD, as the aforementioned advanced transforms, employs samples captured within time domain-based signals in order to developed dedicated $\boldsymbol{U}_0^{-1}\boldsymbol{U}_1$ matrix to solve a so-called generalized eigenvalues problem according to the following formula

$$\mathbf{U}_1\mathbf{B}_k = u_k\mathbf{U}_0\mathbf{B}_k \tag{1}$$

useful to calculate frequencies and amplitudes of the signal, and in which u_k are the eigenvalues and B_k the eigenvectors. Eq. (1) is called as generalized eigenvalues problem. To avoid instability in diagonalization, due to the arising of undesirable peaks in frequency spectrum, DSD employs windowing approach during pre-processing, called band-limited decimation (*bld*), to lower original signal dimension related to matrix of data in order to compute a summation of damped exponentials extracted from the signal under consideration as

$$c_n = \sum_{k=1}^{K} d_k e^{-j\omega_k n\tau} \tag{2}$$

with amplitude d_k and frequency ω_k. Decimated signal diagonalization executes a FFT on time signal $\{cn\}$, having N points with a sampling time

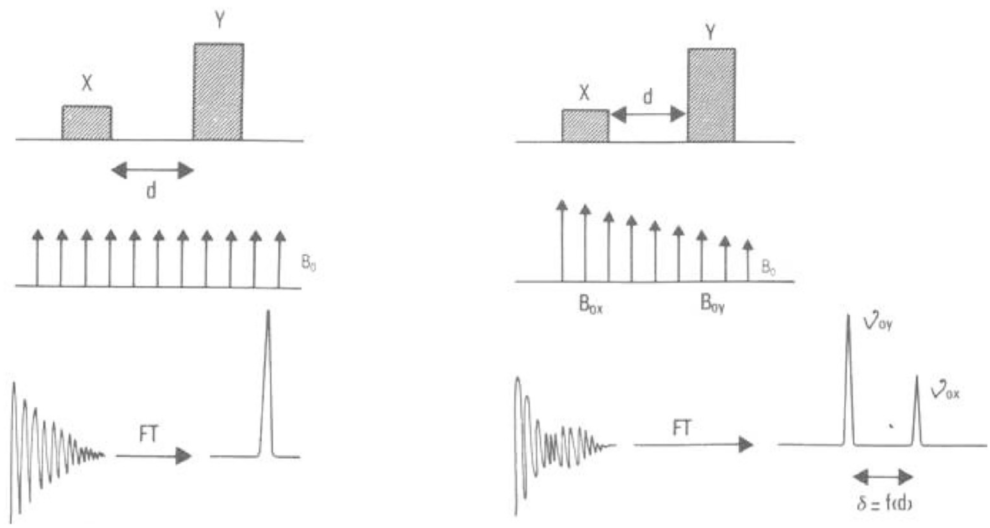

Fig. 4. Frequency coding: MNR in homogeneous field (left), and presence of field gradient (right).

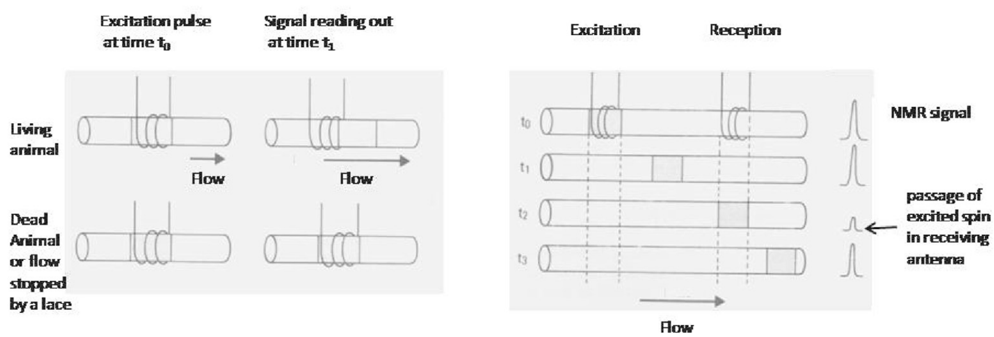

Fig. 5. NMR - based flow measurement.

denoted as τ, to retrieve the Fourier spectrum with low-resolution, such as

$$C_k = \sum_{n=0}^{N-1} c_n e^{j2\pi \frac{n}{N} k}, \quad k = 0, \ldots\ldots, N-1 \tag{3}$$

The spectrum $\{Ck\}$ is divided into $M = N/ND$ frequency windows $[\omega kmin, \omega kmax]$, where $ND = kmax\text{-}kmin + 1$ is the number of points of $\{Ck\}$ contained in each window. So, M decimated band-limited spectra $\{C_k^{bld}\}_{k=0,\ldots,N_d-1}$, are obtained taking into consideration only samples Ck in the chosen window, which are shifted to relocated them symmetrically around the frequency origin $\omega = 0$. Further details are described in Ref. [10]. The 2D DSD algorithm is concisely here below. Now we describe the diagonalization procedure that extracts all of the relevant peak parameters, namely the complex frequencies and amplitudes, $\{\omega_{ik}, d_{ik}\}$, from the window $[\omega_{\min}, \omega_{\max}]$. As with FDM, the DSD technique is restricted to signals that are given as sums of damped exponentials. Therefore, we model the band-limited decimated signal c_n^{bld} as

$$C_n^{bld} = \sum_{k=1}^{K} d_k e^{-jwn\tau_D}, \mathrm{Im}\omega_k < 0 \tag{4}$$

Moreover, like FDM, DSD uses windows to reduce a large data matrix to a number of simple ones before diagonalization. However, while FDM filters basis functions to create its windows, DSD filters the time signal. A time signal is processed to get a low-resolution spectrum by DFT. This spectrum is divided into M windows containing at most 200 data points. A new signal is created for each window by zeroing the content outside the window and then re-centering the window at zero. The inverse DFT is performed to convert the frequency data back into the time domain. The decimation step occurs when this new time signal is sampled at M times greater than the original time step, creating a band-limited decimated signal, which is diagonalized to extract the spectral parameters for the matrix overlapping U_{0d}, U_{1d} and U_{2d}. For each of the M signals implemented, a diagonalization procedure is set, then

$$\begin{aligned} C_{1n}^{bld} &= \sum_{k=1}^{K} d_{1k} e^{-jw_{1k} n\tau_D} \rightarrow U_1 B_{1k} = u_{1k} U_0 B_{1k} \\ C_{2n}^{bld} &= \sum_{k=2}^{K} d_{2k} e^{-jw_{2k} n\tau_D} \rightarrow U_2 B_{2k} = u_{2k} U_0 B_{2k} \end{aligned} \tag{5}$$

The $\omega 1k$ and $\omega 2k$ are extracted from the eigenvalues $u1k = \text{e-j}\omega 1k\tau$ and $u2k = \text{e-j}\omega 2k\tau$ of the operator namely

$$\begin{aligned} \omega_{1k} &= -\frac{1}{\tau_D} \measuredangle(u_{1k}) \\ \omega_{2k} &= -\frac{1}{\tau_D} \measuredangle(u_{2k}) \end{aligned} \tag{6}$$

while the amplitude parameters are calculated as

$$\begin{aligned} d_{1k} &= (0|\omega_{1k})^2 = \left(C_1^T B_{1k}\right)^2 = \left(\sum_{n=0}^{K-1} B_{n1k} C_{1n}^{bld}\right)^2 \\ d_{2k} &= (0|\omega_{2k})^2 = \left(C_2^T B_{2k}\right)^2 = \left(\sum_{n=0}^{K-1} B_{n2k} C_{2n}^{bld}\right)^2 \end{aligned} \tag{7}$$

After that we can calculate the cross-amplitude as

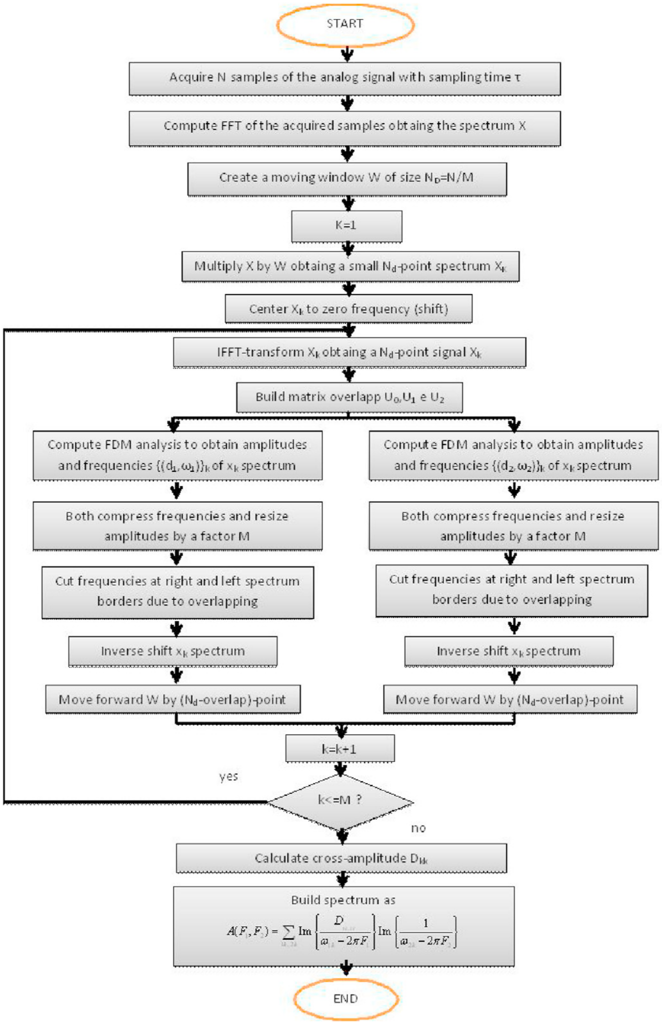

Fig. 6. 2D algorithm for DSD in leak detection.

$$D_{kk} = B_{1k}^T U_0 B_{2k} \sqrt{d_{1k} d_{2k}} \tag{8}$$

and build up bi-spectrum as

$$A(F_1, F_2) = \sum_{1k,2k} \mathrm{Im}\left\{\frac{D'_{1k,2k}}{\omega_{1k} - 2\pi F_1}\right\} \mathrm{Im}\left\{\frac{1}{\omega_{2k} - 2\pi F_2}\right\} \tag{9}$$

The 2D DSD algorithm is summarized in Fig. 6.

It is necessary to note that, with respect to traditional decimation that causes information loss, band-limited decimation, that is used here to preserve information, is envisioned for the overall M windows. BLD (Band-Limited Decimation) only serves to divide the problem under consideration in smallest parts. In the event of narrow windows, that is small N_D, a certain distortion can arise, and this fact has to be taken into account when choosing N_D. As a demonstration, BLD is without information loss, it is simple to note it by means of the analytical expression of the generic sample of $\{c_n^{bld}\}_{k=0,\dots,N_D-1}$:

$$c_n^{bld} = \frac{1}{N} \sum_{n'=0}^{N-1} c_{n'} e^{j2\pi \frac{k_0}{N} n'} \frac{\sin(\pi N_D [n/N_D - n'/N])}{\sin(\pi [n/N_D - n'/N])} \tag{10}$$

where, to build the decimated signal, all samples of the entire signal appear that is $\{c_{n'}\}_{n'=0,\dots,N-1}$, even if that does not mean all samples will give a contribution different from zero. Fig. 7 illustrates sequences of an example of BLD. The signal $\{c_n\}$ is first transformed in frequency domain through FFT. In the spectrum, as instance, a small window (dashed line) is selected that is subsequently centered with respect to $\omega = 0$. Finally, inverse FFT is carried out to obtain the decimated signal $\{c_n^{bld}\}_{k=0,\dots,N_D-1}$.

For each of the M signals $\{c_n^{bld}\}$, it is necessary to launch a diagonalization procedure similar to that used for FDM. Then the $\{c_n^{bld}\}$ is translated into a linear system with generalized eigenvalues as reported in Eq. (5). This almost demanding and detailed discussion, on DSD and its multidimensional approach, is very important since it can help to understand sensor design for, that may capture signals due to decaying process, as it is outlined in this paper.

3. Experimental facility

The main devices of the experimental plant are pressure sensors (Gem 2000), as per Fig. 8, that allow to detect vibrations within the pipeline. The experimental plant, as outlined and represented in Fig. 9, is a hung zigzag pipeline of 120 m (70 m + 50 m), having a diameter of 1 inch. The pressure sensor is manufactured by means of chemical vapour deposition (caption 1) for detection stability and high sensitivity; the case is in stainless steel (caption 2). Electrostatic discharge protection circuit is provided (caption 3), and to increase linearity, an ASIC chip is included (caption 4), and a thicker diaphragm for managing pulsating pressures is encompassed (caption 5). Water is extracted from a tank and pumped within the pipeline.

Eleven valves are also installed to simulate leaks. A computerized system is able to supervise the operating mode of the facility allowing to receive and control signals from sensors. Any other detail regarding hydraulic circuit and statistical treatment are included in Ref. [10].

A zigzag plant is a complex version of a traditional pipeline or waterworks insofar as it encompasses difficult operating modes. Hence, the facility includes conditions where water is pumped from low altitude to high altitude and vice versa.

4. Data acquisition and results

A real time acquisition architecture is provided, taking signal from sensors with appropriate conditioning circuits and controller (PICPLC 16), allowing a processing by means of a computer equipped with a Matlab environment. Fig. 10 shows a typical GUI with diverse possibilities to run programs connected to FDM, and DSD. Within the same GUI, attention must be paid on eigenvalues representation that gives us stability in the solution of the generalized eigenvalues problem according to Eq. (1) that impacts on the aforementioned equations (from Eq. (5) To Eq. (9)) due to the presence of matrix $\boldsymbol{B}$. For acquisitions, as captured by the sensor illustrated in Fig. 11 (a), the value of pressure is displayed (Fig. 11 (b)); sensor connections are illustrated in Fig. 11 (c) and different peaks are reported in Fig. 11 (d). As per the scope of this paper, 1D representation fulfils the objectives of leak detection but a 2D/3D representation is useful to know what happens within the pipe and which areas/points of the pipe are strongly under stress. Spatial illustration is very important to also understand inner pipe saturation due to eventual air trapped inside. In some waterworks micro-cameras are usually located in strategic points to monitor spatial distribution of water flow. The proposed 2D/3D sensing approach can act in lieu of micro-cameras even in aqueous harsh environments, as instance sludge waters.

For sludge waters, cameras are inappropriate, and this kind of proposal is suitable for the scope.

Recalling stress, in case of persisting pressure, for buried pipes and/or pipes constrained in the underneath part, in the event of leak in the top part, there would not be useful to remove the part of the pipe torso but just repairing the hole/holes; as if we had a camera to localize hole and/or crack.

There is an important question in pipeline maintenance: not only detecting the leak but also its quality: hole, crack, etc. In Figs. 12–14, we report 2D/3D representation of the leak for water taps 1,4, and 10 respectively. The water taps are related to the above hydraulic circuit.

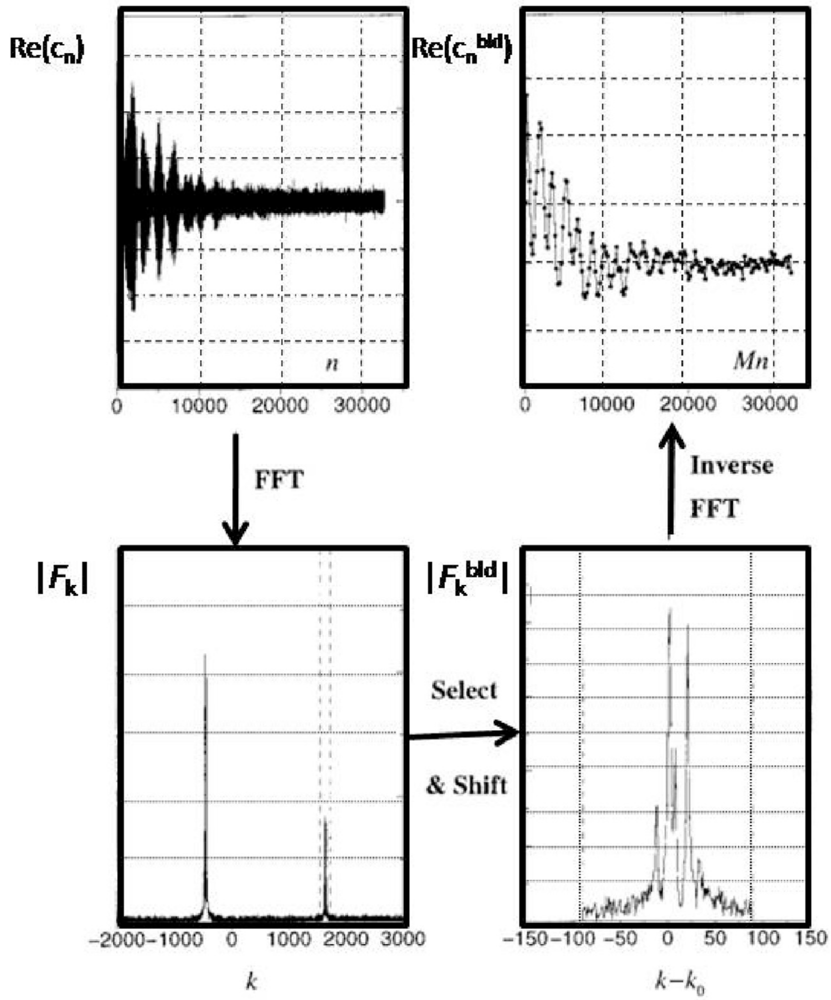

Fig. 7. Band-limited decimation principle.

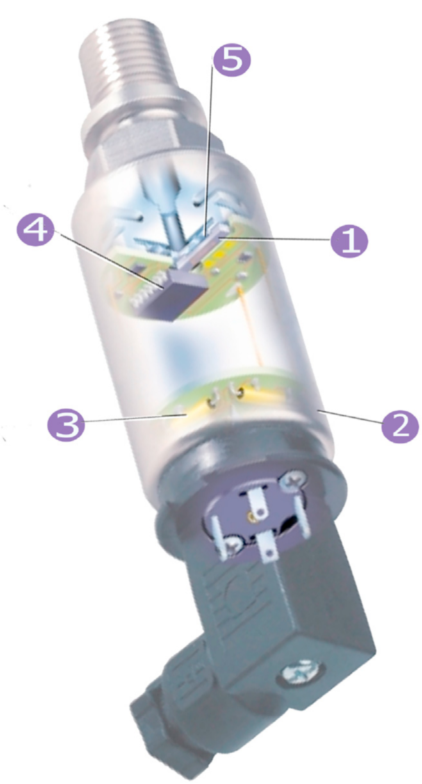

Fig. 8. Pressure sensor piece parts.

Each Figure (any of 1,4, and 10) represents the amplitude (in volt) or magnitude (in bar) in vertical axis along with length and width of leak in *xz* plane. On the right of each Figure we include eigenvalues representation related to the inversion of calculated matrices of Eq. (1). This inversion is also a key issue in FDM and DSD. In case of ill-posed problem due to difficulties in matrix inversion, some eigenvalues will be outside the circle. However, this cannot happen here because we have implemented an algorithm based on *L-curve* technique [11]. Notice that we have taken three significant cases. When peaks family is located in the center and close to *x* axis, there are few eigenvalues in the inner area of the circle as reported in Fig. 12; on the contrary, if the peaks family is far from *x* axis, there is an increase of eigenvalues in the inner area of the circle, see Fig. 14. Fig. 13 is a so-called drawback. Moreover, since DSD partly leverages the same approach of FDM, both algorithms can be compared for the experimental circuit; that is in terms of ME (Mean Error), MSE (Mean Squared Error), RMSE (Root Mean Squared Error), and computational time to recover a leak. We reaffirm best performances of DSD with respect to FDM for low frequency signals as reported in Fig. 15.

In normal conditions of flow, without a sudden opening of water taps that simulate leaks, the sensors along with the processing are able to help for detecting the normal flow. Using 3D DSD, we are able to illustrate the flow using cross-amplitude representation included in 3D DSD algorithm. Fig. 16 demonstrates both cross-amplitude and the top-view of pressure within the pipeline. That is to testify the importance of this imaging in order to know mechanical stress the pipeline is undergoing with. It is also important to know the leak detection time. According to Fig. 17,

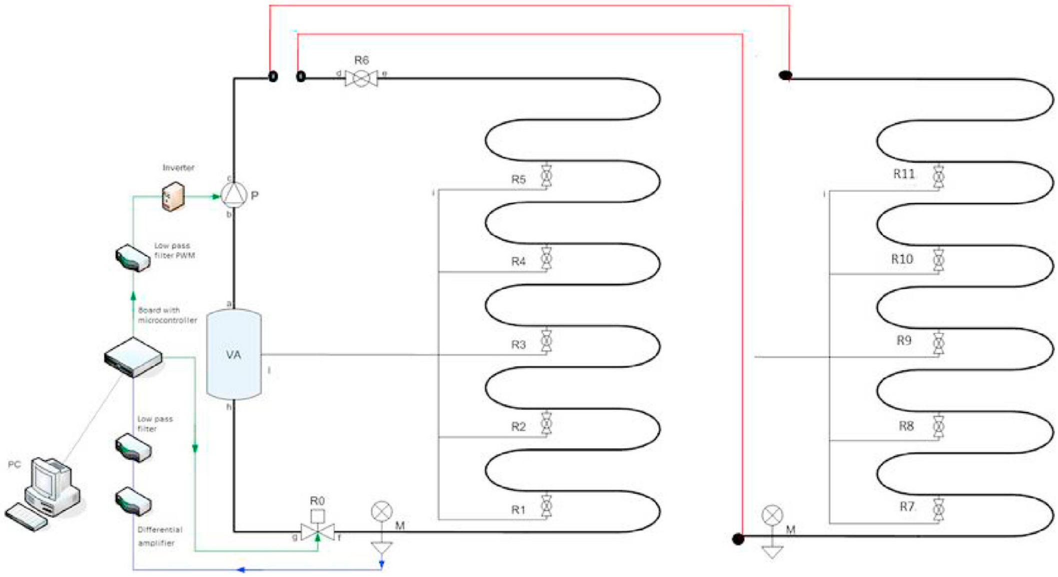

Fig. 9. Experimental hydraulic circuit with both partial circuits of 70 m and 50 m respectively.

detection times of leaks (see useful peaks) are 16 s for leak 1, 19 s for leak 2, 28 s for leak 3, and 42 s for leak 4. This time is increasing because water tap 1 is close to the first sensor.

Now we are ready to show leak detection in function of distance from the first sensor and its uncertainty. Table 1 illustrates these results. Uncertainty is significant for ascending leaks. In other words, when water is from low share to up share. This torso is 70 m long; but the descending torso, with leaks from 7 to 11 exhibits a low uncertainty. This difference may be due to roughness offered by the pipeline. We need two working frequencies, as reported in Fig. 16, to detect the peak. The uncertainty is

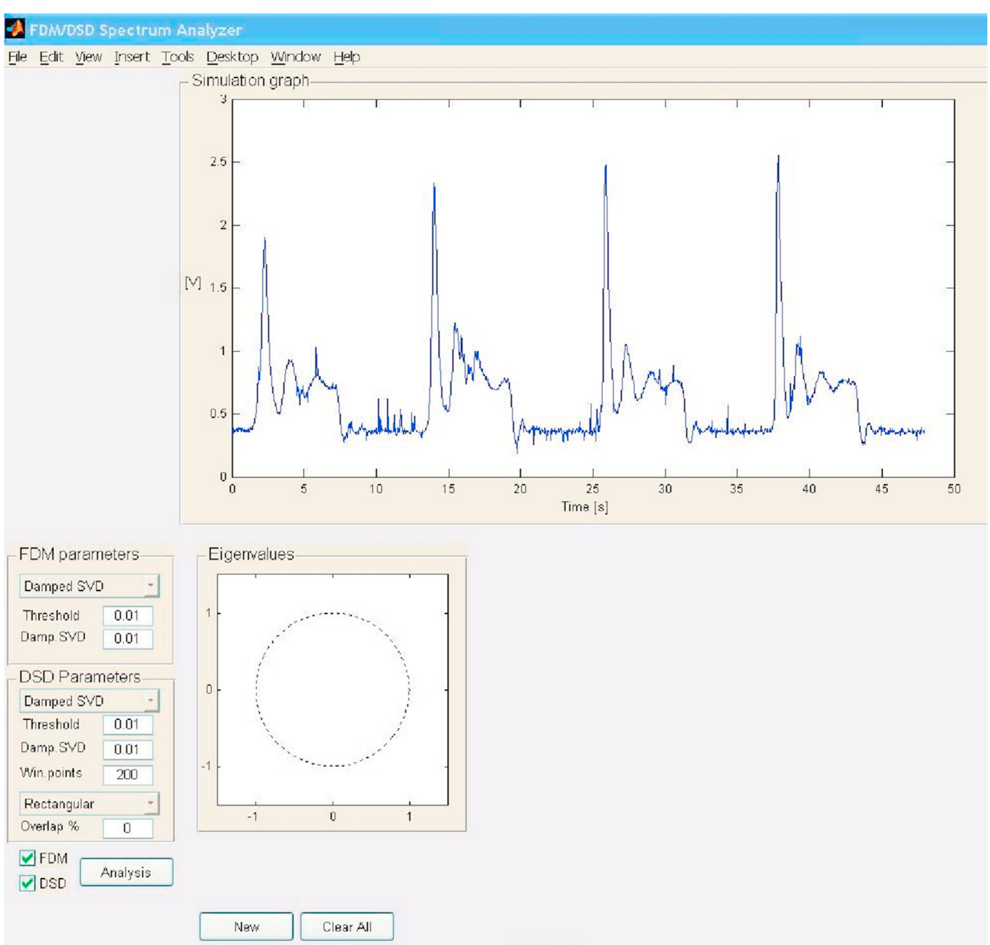

Fig. 10. Graphical unit interface (GUI) for acquiring and processing signals delivered by sensors.

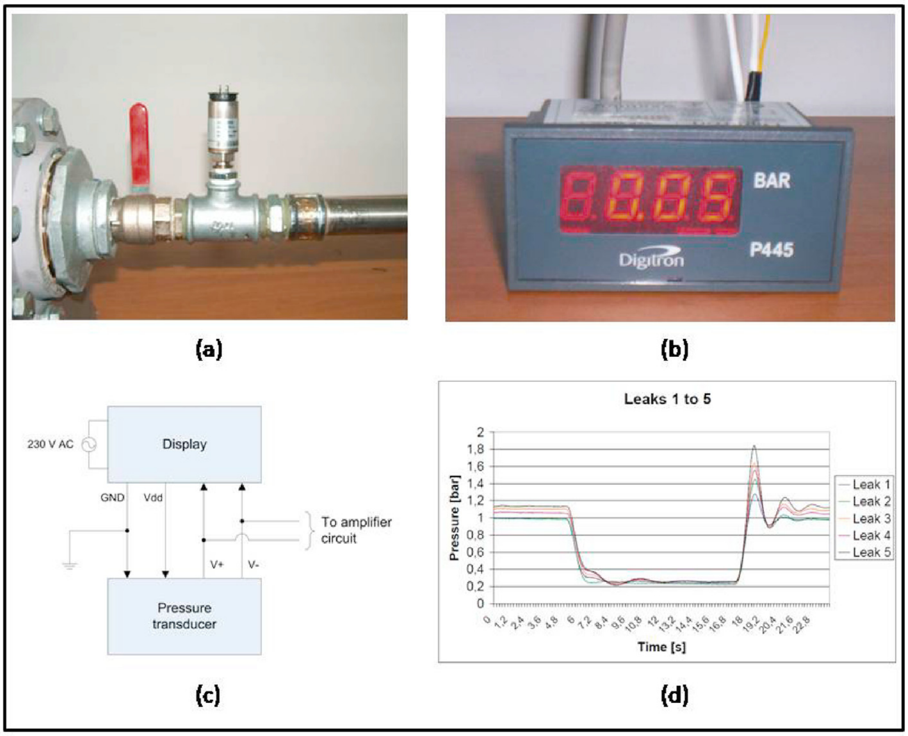

Fig. 11. Sensing system mounted on pipe and acquisitions.

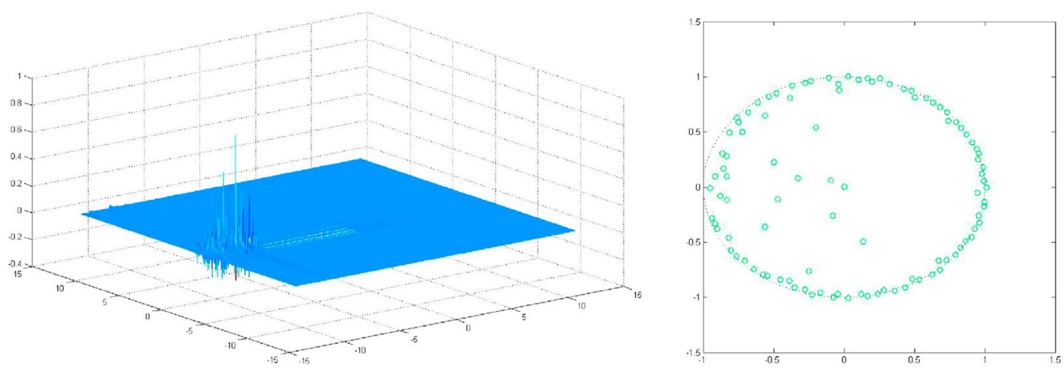

Fig. 12. Leak 1 corresponding to water tap 1 represented within the pipeline as 3D distribution of pressure amplitude (*y*/vertical), *xz* plane in length/width (a) and traced out eigenvalues circle (b).

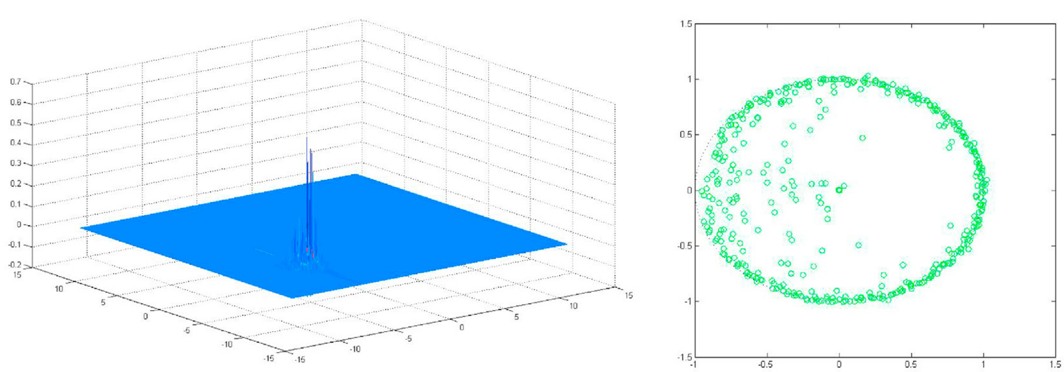

Fig. 13. Leak 4 corresponding to water tap 4 represented within the pipeline as 3D distribution of pressure amplitude (*y*/vertical), *xz* plane in length/width (a) and traced out eigenvalues circle (b).

here intended how is range of detecting the right position of the leak. For example leak 1 is detected at 57.2 $\pm$ 3.84 m with linear regression computation and 57.2 $\pm$ 5.48 m with quadratic regression. Of course, for non zigzagging and hung pipeline, we mean a linear waterworks, the uncertainty could be around 5 $\div$ 6 times less than that here encountered. This is also an excellent finding.

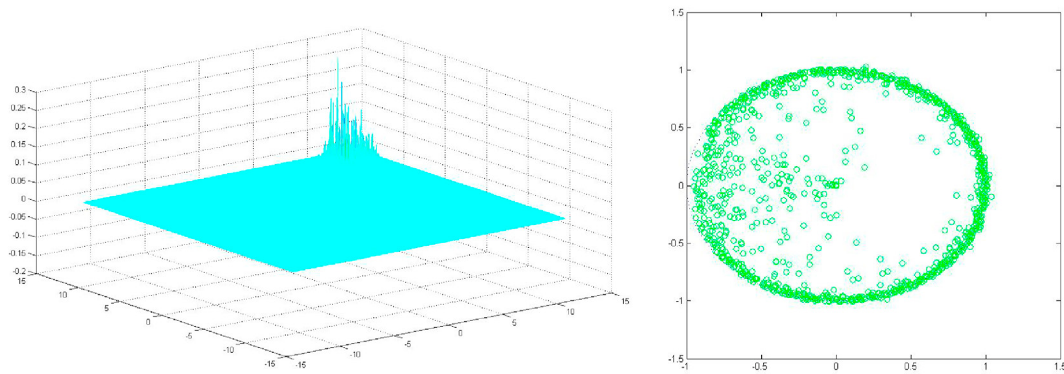

Fig. 14. Leak 10 corresponding to water tap 10 represented within the pipeline as 3D distribution of pressure amplitude (*y*/vertical), *xz* plane in length/width (a) and traced out eigenvalues circle (b).

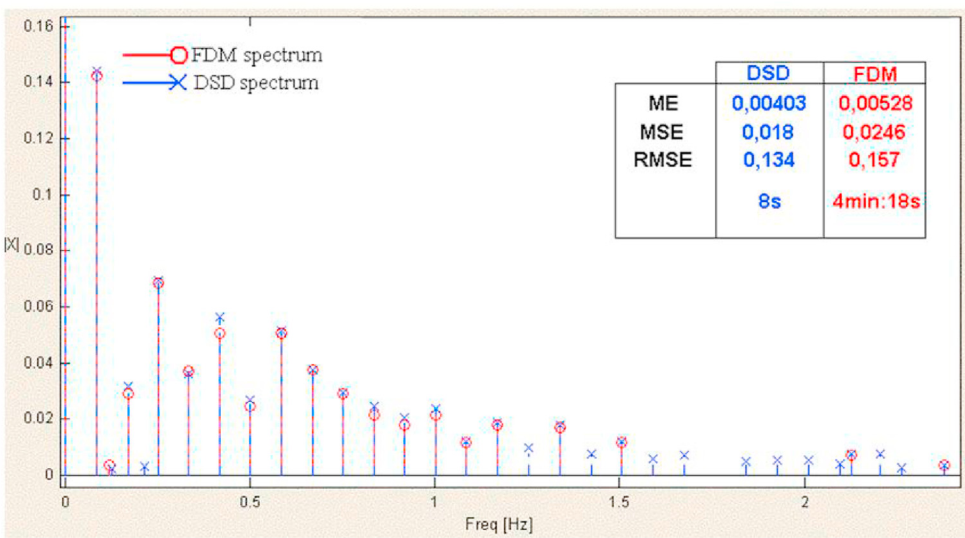

Fig. 15. Performance comparisons and metrics for DSD and FDM.

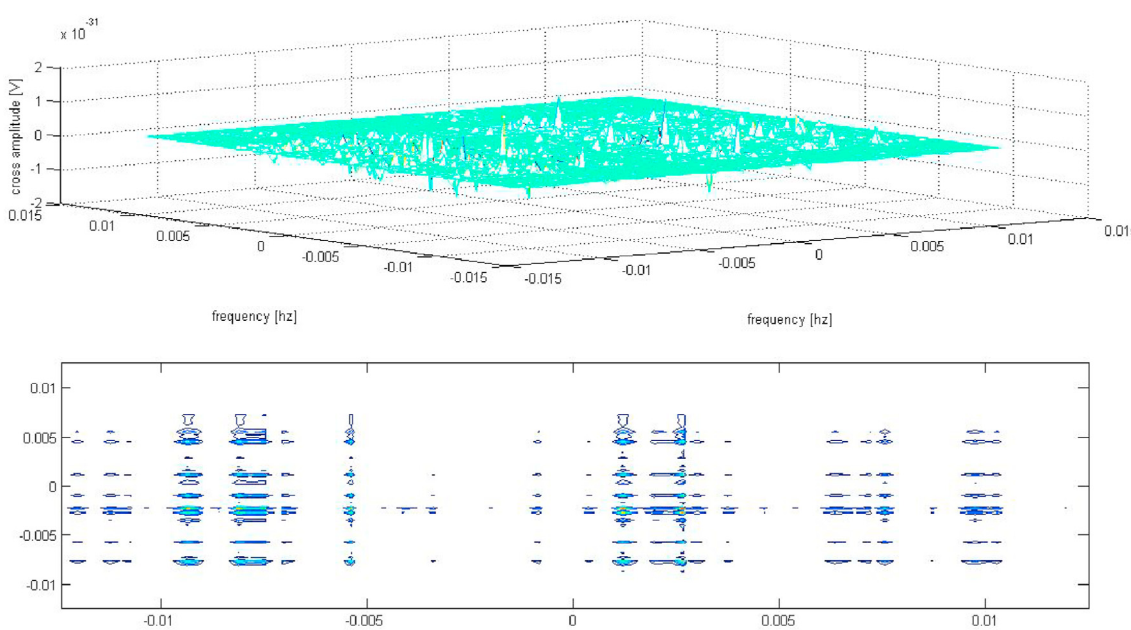

Fig. 16. Leak 10 cross-amplitude in normal conditions (up) and top-view (down) of flow within the pipeline.

We have recalled NMR approach to retrieve leaks since it is necessary to transform signals from time domain into frequency domain. In reality, as it is done for humans and animals by using NMR and DSD/FDM techniques to recover signal [12,13], it is possible to envision peaks

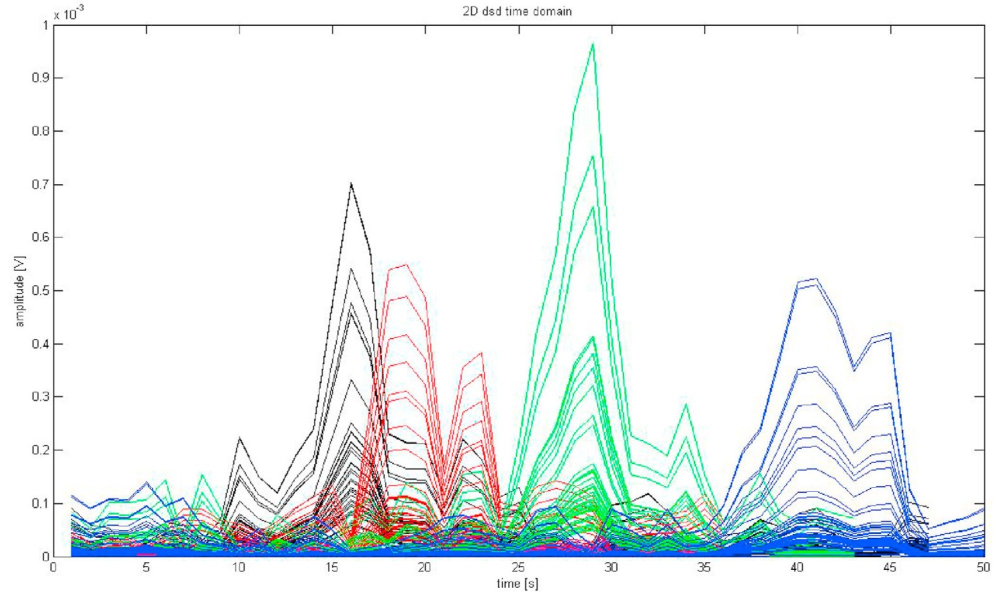

Fig. 17. Detection time and peak for leaks from 1 to 4.

Table 1
Uncertainty retrieved using 2D DSD.

Leak	Work ing frequency [Hz; Hz]	Half width peak [Hz]	Distance [m]	Uncertainty with linear regression	Uncertainty with quadratic regression
1	(0; 1.02)	0.1414	57.2	±3.84	±5.48
2	(0; 1.02)	0.1133	47.7	±3.84	±5.48
3	(0; 1,02)	0.1047	38.2	±3.84	±5.48
4	(0; 1.02)	0.0922	28.7	±3.84	±5.48
5	(0; 1.02)	0.0873	18.2	±3.84	±5.48
6	(0; 1.02)	0.0601	9.7	±3.84	±5.48
7	(0; 0.39)	0.0031	1.85	±1.04	±0.60
8	(0; 0.39)	0.0063	9.85	±1.04	±0.60
9	(0; 0.39)	0.0091	17.85	±1.04	±0.60
10	(0; 0.39)	0.0131	25.85	±1.04	±0.60
11	(0; 0.39)	0.0175	33.85	±1.04	±0.60

within the pipeline (Fig. 18) as it happens within human/animal muscles, arteries and veins.

5. Conclusions

Advanced transforms may find applications in many fields of Engineering given the fact they are used in Medicine and Physics. They mostly deal with vibrations derived from diverse natures namely: brownian motion, thermal agitation, etc., that may include decaying process. In this perspective, Decimated Signal Diagonalization (DSD) is a nonlinear spectral estimation technique, as FDM, exhibiting more advantages than FFT and STFT. DSD, as FDM, expresses a summation of complex smoothed signals with high capability to resolve peaks as illustrated in Fig. 19; FFT and STFT do not. Moreover DSD exploits decimation and diagonalization. Decimation has been already explained in the previous section 2. But diagonalization is an important an undeniable plus since only diagonal matrices commute in lieu of matrix multiplication [14,15].

The combination of decimation and diagonalization tributes a powerful capability to DSD to treat oscillating motion due to vibrations trapped in a fluid, as instance water. These vibrations, within a decaying process, suffer from collisional motions with impact on observational time and frequency. The need of frequency coding may amplify signals coming from sensors able to capture these collisional motions even in

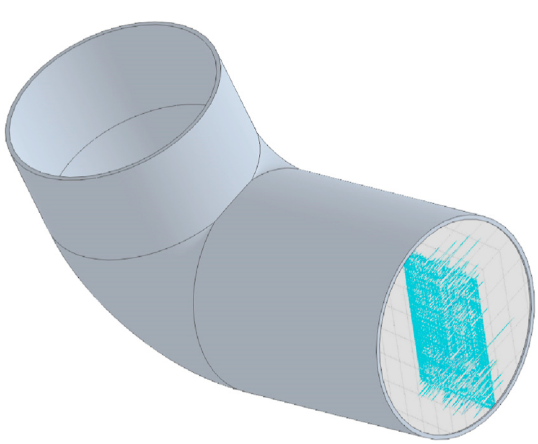

Fig. 18. 3D representation of peaks within pipe.

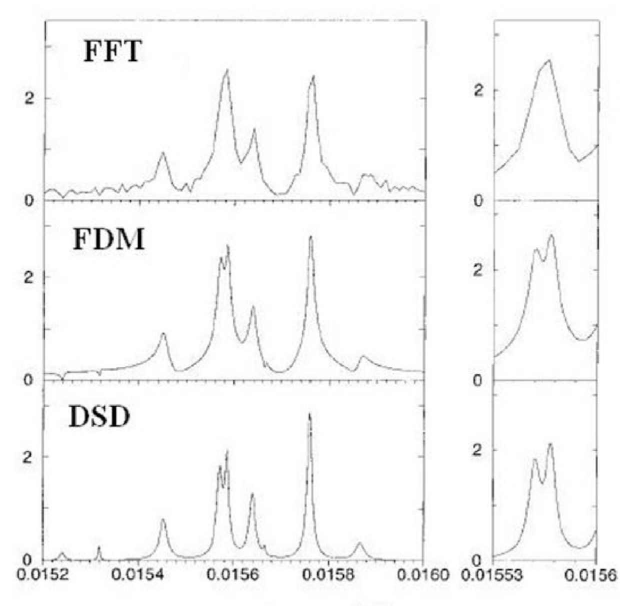

Fig. 19. DSD, FDM and FFT differences in terms of peak resolution.

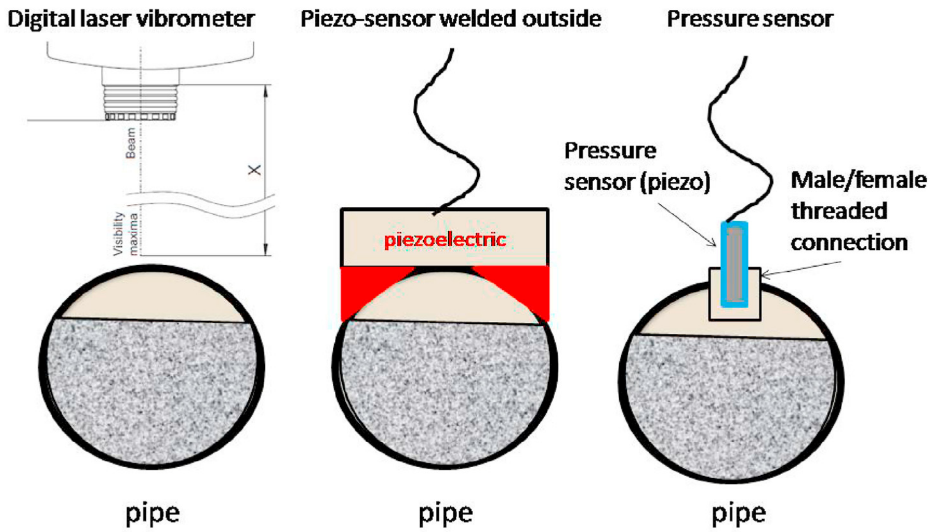

Fig. 20. Some configurations for better using advanced transforms such as DSD as per Fig. 5.

presence of decay mechanisms of dephasing. That is why DSD is strongly apt to display vibrations, for our cases, coming from pipelines by using different sensing modalities as demonstrated in Fig. 20 where it is possible to see three cases: the first (left) is leak/flow regime captured by a laser vibrometer [16], the second is related to a piezoelectric sensor welded on the pipe outer, and the third is faced in this paper.

This work is a step forward with respect to Ref. [10]; as better reported in section 4, we have implemented an imaging approach without using micro-cameras located inside key point of the pipelines. The results are similar to those obtainable by means of a beamforming imaging. But in beamforming we need at least two sensors whilst for this case we only employ one sensor and we leverage the pipe inner torso as a reflector acting also as pseudo-detector.

However, DSD is not only a technique of processing certain types of signals delivered by sensors, but vice versa, it can help the designing of sensors/transducers that can highlight signal contents.

CRediT authorship contribution statement

Aimé Lay-Ekuakille: Conceptualization, Methodology, Software, Data curation, Writing - original draft, Visualization, Investigation, Supervision, Software, Writing - review & editing, Validation. **Vito Telesca:** Validation, Writing - review & editing, Validation.

Declaration of competing interest

The authors declare that they have no known competing financial interests or personal relationships that could have appeared to influence the work reported in this paper.

References

[1] The European Federation of National Water Services, Europe's Water in Figures: an Overview of the European Drinking Water and Waste Water Sectors, 2017 edition, 2008.
[2] S. Sharma, Performance Indicators of Water Losses in Distribution System, UNESCO-IHE, Delft, 2008.
[3] K. Marmarokopos, D. Doukakis, G. Frantziskonis, M. Avlonitis, Leak detection in plastic water supply pipes with a high signal-to-noise ratio accelerometer, Measure. Control 51 (1–2) (2018) 27–37.
[4] P.J. Lee, et al., Frequency domain analysis of pipe fluid transient behaviour, J. Hydraul. Res. 51 (6) (2013) 609–622.
[5] Z. Kapelan, D. Savic, G. Walters, D. Covas, N. Graham, C. Maksimovic, An Assessment of the Application of Inverse Transient Analysis for Leak Detection: Part I - Theoretical Considerations, Computer Control for Water Industry (CCWI), London, UK, 2003.
[6] A. Lay Ekuakille, G. Vendramin, A. Trotta, Spectral analysis of leak detection in a zigzag pipeline: a filter diagonalization method - based algorithm application, Measurement 42 (3 April) (2009) 358–367.
[7] A. Lay-Ekuakille, G. Vendramin, A. Trotta, Robust spectral leak detection of complex pipelines using filter diagonalization method, IEEE Sensor. J. 9 (11) (2010) 1605–1614.
[8] A. Lay-Ekuakille, P. Vergallo, G. Griffo, A robust algorithm based on decimated Padé approximant technique for processing sensor data in leak detection in waterworks, IET Sci. Meas. Technol. 7 (5) (2013) 256–264.
[9] A. Lay-Ekuakille, L. Fabbiano, G. Vacca, J. Kidiamboko Kitoko, P. Bibala Kulapa, V. Telesca, A comparison between decimated Padé approximant and decimated signal diagonalization methods for leak detection in pipelines equipped with pressure sensors, Sensors MDPI 18 (6) (2018) 1–18.
[10] A. Lay-Ekuakille, P. Vergallo, Decimated signal diagonalization method for improved spectral leak detection in pipelines, IEEE Sensor. J. 14 (6) (2014) 1741–1748.
[11] A. Lay-Ekuakille, G. Griffo, P. Visconti, P. Primiceri, R. Velazquez, Leaks detection in waterworks: comparison between STFT and FFT with an overcoming of limitations, Metrol. Meas. Syst. 24 (4) (2017) 631–644.
[12] J.R. Singer, Blow flow rates by nuclear magnetic resonance measurements, Science 130 (1959) 1652–1653.
[13] S.-I. Han, O. Marseille, C. Gehlen, B. Blumich, Rheology of blood by NMR, J. Magn. Reson. 152 (2001) 87–94.
[14] M. Carrasco, J.-P. Florens, E. Renault, Linear inverse problems in structural econometrics estimated based on spectral decomposition and regularization, in: Handbook Econom., 6, 2003. Canada.
[15] T.S. Jang, H.S. Choi, T. Kinoshita, Numerical experiments on an ill-posed inverse problem for a given velocity around a hydrofoil by iterative and noniterative regularizations, J. Mar. Sci. Technol. 5 (3) (2001) 107–111. Springer Japan.
[16] G. Dinardo, L. Fabbiano, G. Vacca, A. Lay-Ekuakille, Vibrational signal processing for characterization of fluid flows in pipes, Measurement 113 (2018) 196–204.